

***AB INITIO* NO CORE METHODS: APPLICATIONS TO LIGHT NUCLEI**

JAMES P. VARY

*Department of Physics and Astronomy, Iowa State University,
Ames, IA 50011, USA
jvary@iastate.edu*

PIETER MARIS

*Department of Physics and Astronomy, Iowa State University,
Ames, IA 50011, USA
pmaris@iastate.edu*

ANDREY SHIROKOV

*Skobeltsyn Institute of Nuclear Physics, Moscow State University,
Moscow, 119991 Russia
shirokov@nucl-th.sinp.msu.ru*

We introduce a no-core full configuration (NCFC) approach and present results for ${}^4\text{He}$, ${}^{12}\text{C}$, ${}^{14}\text{F}$ and some other nuclei with the realistic NN interaction, JISP16. We obtain ground state energies and their uncertainties through exponential extrapolations that we demonstrate are reliable in ${}^4\text{He}$ where fully converged results are obtained. We find ${}^{12}\text{C}$ is overbound by 1.7 MeV and we predict the yet-to-be-measured binding energy of ${}^{14}\text{F}$ to be 70.2 ± 3.5 MeV. The extrapolated spectrum of ${}^{14}\text{F}$ is in reasonable agreement with known features of the ${}^{14}\text{B}$ spectrum. Distinctions are drawn between this approach and the no-core shell model (NCSM).

1. Introduction and Motivation

The rapid development of *ab-initio* methods for solving finite nuclei has opened a range of nuclear phenomena that can be evaluated to high precision using realistic nucleon-nucleon (NN) and three-nucleon (NNN) interactions. Such advances define a path for testing fundamental properties of the strong interaction such as their origins from QCD via chiral effective field theory.^{1–4} In addition, they prepare a foundation for nuclear reaction theory with unprecedented predictive power.

Here we investigate the direct solution of the nuclear many-body problem by diagonalization in a sufficiently large basis space that converged binding energies are accessed - either directly or by simple extrapolation. Our choice is a traditional harmonic oscillator (HO) basis so there are two basis space parameters, the harmonic oscillator energy $\hbar\Omega$ and the many-body basis space cutoff N_{max} . N_{max} is defined as the maximum number of total oscillator quanta allowed in the many-

body basis space above the minimum for that nucleus. We obtain convergence in this 2-dimensional parameter space $(\hbar\Omega, N_{\max})$, where convergence is defined as independence of both parameters within evaluated uncertainties.

Since we treat all nucleons equivalently and we achieve convergence within evaluated uncertainties, we refer to our approach as the “No-Core Full Configuration” (NCFC) method. The NCFC is both related to and distinct from the No-Core Shell Model (NCSM),⁵ that features a finite matrix truncation, and an effective Hamiltonian renormalized to that finite space. The regulator, N_{\max} , appears in our NCFC, where it is taken to infinity, and in the NCSM, where it also appears in the definition of the effective Hamiltonian. In both NCFC and NCSM, this choice of many-body basis regulator, N_{\max} , is needed to preserve Galilean invariance - to factorize all solutions into a product on intrinsic and center-of-mass motion components. With N_{\max} as the regulator, both the NCFC and the NCSM are distinguished from the “Full Configuration Interaction” (FCI) method in atomic and molecular physics that employs a cutoff in single-particle-space.

The NCFC results should agree with the NCSM and no-core FCI results when the latter results are obtained in sufficiently large basis spaces. In the case of NCSM, larger cluster sizes for the effective Hamiltonian may be employed to accelerate convergence.

2. Hamiltonian Ingredients, Basis Selection and Method of Solution

In order to carry out the NCFC calculations, we require a realistic NN interaction that is sufficiently weak at high momentum transfers that we can obtain a reasonable convergence trend. The conventional Lee–Suzuki–Okamoto renormalization procedure of the *ab-initio* NCSM⁵ develops effective interactions that provide answers close to experimental observations. However, the convergence trend of the effective interaction sequences with increasing N_{\max} is not uniform and leads to challenges for extrapolation. Therefore, we select the realistic NN interaction, JISP16, that produces spectra and other observables in light nuclei that are already known to be in reasonable accord with experiment.⁶

In order to further motivate our efforts to develop robust extrapolation tools, we show in Fig. 1 the Hamiltonian matrix dimensions for a set of representative light nuclei. The nearly exponential growth in matrix dimension with increasing N_{\max} is clearly evident in Fig. 1. In order to achieve NCFC results for the heavier of these nuclei by extrapolation, using realistic interactions, we would need to diagonalize matrices that are beyond the reach of present technologies. However, in cases up to and including ^{16}O , we may expect to obtain systematic results for the first few increments of N_{\max} . In order to use the sequence obtained with N_{\max} values that are currently accessible, we need to investigate suitable extrapolation tools.

We employ the “m-scheme” where each HO single-particle state has its orbital and spin angular momenta coupled to good total angular momentum, j , and mag-

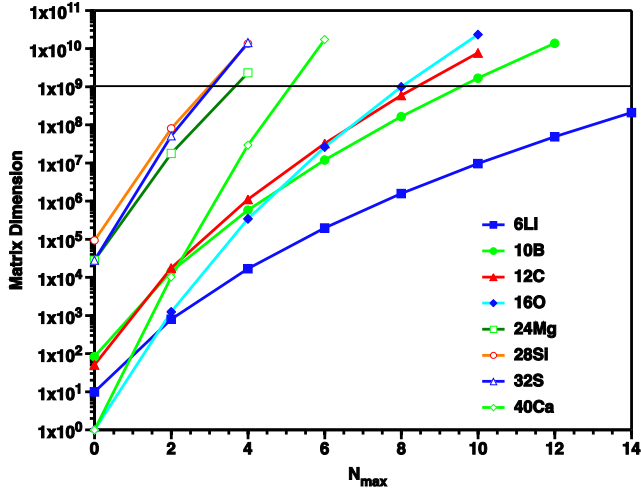


Fig. 1. (Color online) Representative Hamiltonian matrix dimensions for total magnetic projection $M = 0$ states in the single-particle m-scheme as a function of the oscillator quanta of excitations specified by N_{\max} . The natural parity matrix dimensions are represented by the specific points while unnatural parity matrix dimensions would lie close to the interpolating lines at odd values of N_{\max} . The horizontal bar indicates the matrix dimension 1 billion. We achieve results with basis dimension of nearly 2 billion in this work.

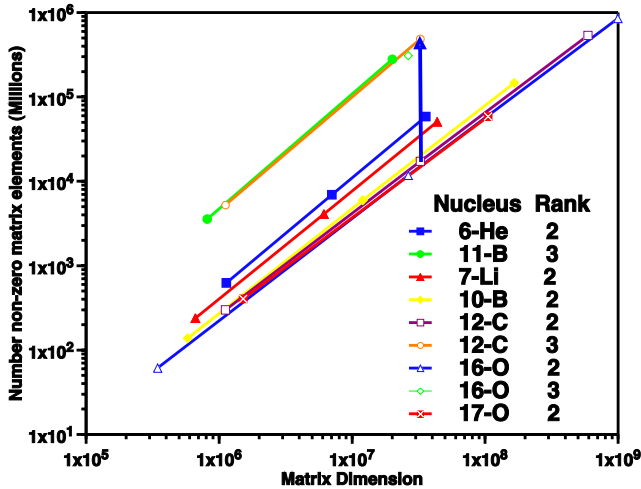


Fig. 2. (Color online) Number of non-vanishing many-body Hamiltonian matrix elements for representative light nuclei as a function of the basis space dimension. The points represent sample cases that have been solved and correspond to those indicated in the legend. The curves approximate a $D^{3/2}$ power law where D is the basis space dimension. The vertical arrow measures a factor of 30 between the 2-body Hamiltonian (rank=2) and 3-body Hamiltonian (rank=3) cases for ^{12}C at the same dimension corresponding to $N_{\max} = 6$. Note the logarithmic scales.

netic projection, m . The many-body basis states are Slater determinants in this HO basis and are limited by the imposed symmetries - parity and total angular momentum projection (M), as well as by N_{\max} . In the natural parity cases for even (odd) nuclei, $M = 0$ ($M = \frac{1}{2}$) enables the simultaneous calculation of the entire spectrum for that parity and N_{\max} .

To better understand the scale of computational effort needed for no-core microscopic nuclear structure studies, we consider the memory storage demands as a function of matrix dimension. For several representative nuclei, we enumerate the number of non-vanishing matrix elements of the resulting many-body Hamiltonian matrix (lower diagonal only for efficiency) and display the resulting counts as a function of the matrix dimension in Fig. 2. We present results for the case of a 2-body input Hamiltonian (NN interaction only) and for the case of a 3-body Hamiltonian (NN + NNN interactions). In spite of the very large memory requirements, the various curves display an encouraging trend. Specifically, the number of non-vanishing many-body matrix elements follows a $D^{3/2}$ growth rate, where D is the dimension of the matrix. That is, the matrices exhibit a very sparse character and this is the property that allows us to diagonalize the large matrices that we can presently solve.

We employ the code “Many Fermion Dynamics — nuclear” (MFDn)⁷ that evaluates the many-body Hamiltonian and obtains the low-lying eigenvalues and eigenvectors using the Lanczos algorithm.

In the NCFC approach discussed here, we seek to obtain the ground state energy of the original Hamiltonian in the infinite model space with evaluated uncertainties. To this end, we incorporate systematic and reliable extrapolation tools as needed. Note that we do not use a renormalized Hamiltonian such as one obtained from the Lee–Suzuki–Okamoto method employed with the NCSM.

By investigating the calculated binding energies of many light nuclei as a function of the two basis space parameters, we determined that, once we exclude the $N_{\max} = 0$ result, the calculated points represent an exponential convergence pattern at fixed $\hbar\Omega$. Therefore, we fit an exponential plus constant to each set of results as a function of N_{\max} , excluding $N_{\max} = 0$, at fixed $\hbar\Omega$, using the relation:

$$E_{\text{gs}}(N_{\max}) = a \exp(-cN_{\max}) + E_{\text{gs}}(\infty). \quad (1)$$

3. Extrapolating the Ground State Energy — NCFC Test Cases with ${}^4\text{He}$

We now investigate the convergence rate for the ground state energy as a function of N_{\max} and $\hbar\Omega$ for ${}^4\text{He}$ where we also achieve nearly exact results by direct diagonalization for comparison. In particular, we present the results and extrapolation analyses for ${}^4\text{He}$ in Figs. 3 through 5.

The sequence of curves in Fig. 3 for ${}^4\text{He}$ illustrates the trends we encounter in our calculations when evaluating the ground state energy with the “bare” JISP16 interaction. Our purpose with ${}^4\text{He}$ is only to illustrate convergence trends. The

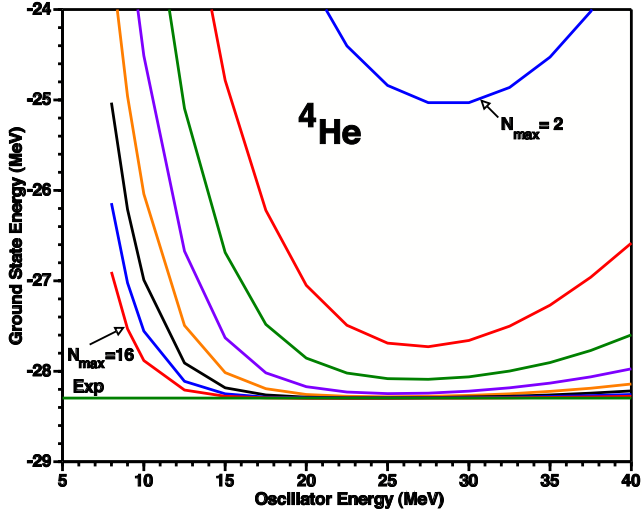


Fig. 3. (Color online) Calculated ground state energy of ${}^4\text{He}$ as a function of the oscillator energy, $\hbar\Omega$, for a sequence of N_{max} values. The curve closest to experiment corresponds to the value $N_{\text{max}} = 16$ and successively higher curves are obtained with N_{max} decreased by 2 units for each curve.

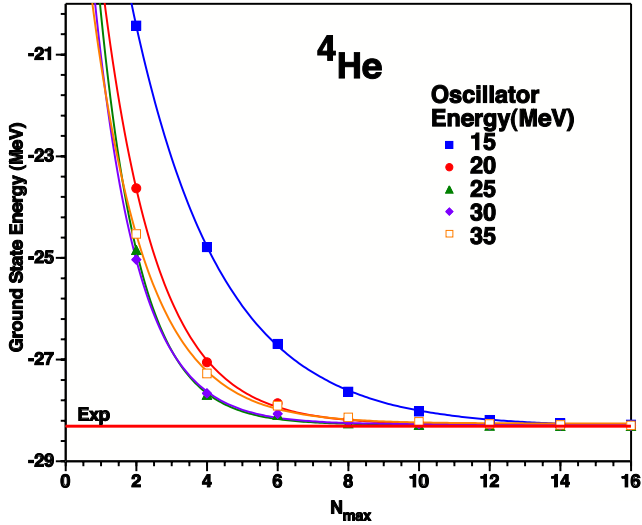


Fig. 4. (Color online) Calculated ground state energy of ${}^4\text{He}$ for $N_{\text{max}} = 2-16$ for JISP16 at selected values of $\hbar\Omega$. Each set of points at fixed $\hbar\Omega$ is fitted by Eq. (1) producing the solid curves. Note the expanded energy scale. Each point is a true upper bound to the exact answer. The asymptotes $E_{\text{gs}}(\infty)$ are the same to within 35 KeV of their average value and they span the experimental ground state energy.

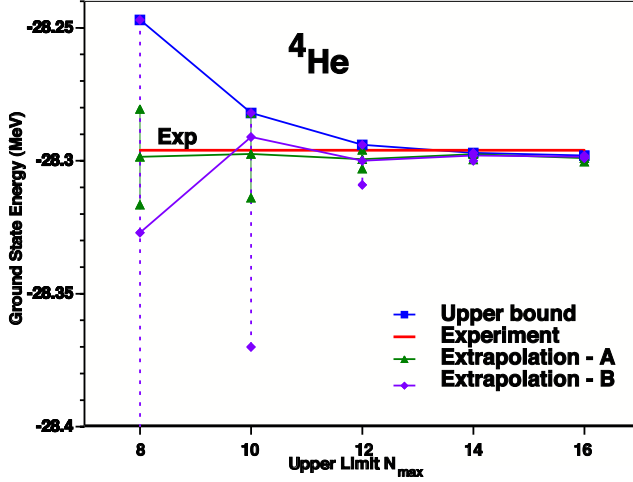


Fig. 5. (Color online) Extracted asymptotes and upper bounds as functions of the largest value of N_{\max} in each set of points used in the extrapolation. Four (three) successive points in N_{\max} are used for the extrapolation A (B). Uncertainties are determined as described in the text. Note the expanded scale and the consistency of the asymptotes as they fall well within their uncertainty ranges along the path of a converging sequence.

$N_{\max} = 18$ results (not shown) reach to within 3 KeV of the exact answer that agrees well with experiment.

Next, we use these ${}^4\text{He}$ results to test our “extrapolation method A” as illustrated in Fig. 4. For extrapolation A, we will fit only four calculated points at each value of $\hbar\Omega$. However, in Fig. 4 we demonstrate the exponential behavior over the range $N_{\max} = 2-16$. Later, we will introduce a variant, “extrapolation method B” in which we use only three successive points for the fit. For extrapolation A, we select the values of $\hbar\Omega$ to include in the analysis by first taking the value at which the minimum (with respect to $\hbar\Omega$) occurs along the highest N_{\max} curve included in the fit, then taking one $\hbar\Omega$ value lower by 5 MeV and three $\hbar\Omega$ values higher by successive increments of 5 MeV. For heavier systems we take this increment to be 2.5 MeV. Since the minimum occurs along the $N_{\max} = 16$ curve at $\hbar\Omega = 20$ MeV as shown in Fig. 3, this produces the 5 curves spanning a range of 20 MeV in $\hbar\Omega$ shown in Fig. 4.

We recognize that the selected window of results in $\hbar\Omega$ values is arbitrary. Our only assurance is that our selection appears to provide a consistent set of extrapolations in the nuclei examined up to the present time.

For the resulting 5 cases shown in Fig. 4, we employ an independent exponential plus constant fit for each sequence, perform a linear regression for each sequence at fixed $\hbar\Omega$, and observe a small spread in the extrapolants that is indicative of the uncertainty in this method. Note that the results in Fig. 4 are obtained with equal weights for each of the points.

For extrapolation A, we will fit sets of 4 successive points due to a desire to minimize the fluctuations due to certain “odd-even” effects. These effects may be interpreted as sensitivity to incrementing the basis space with a single HO state at a time while including two successive basis states affords tradeoffs that yield a better balance in the phasing with the exact solution.

Next, we consider what weight to assign to each calculated point. We argue that, as N_{\max} increases, we are approaching the exact result from above with increasing precision. Hence, the importance of results grows with increasing N_{\max} and this should be reflected in the weights assigned to the calculated points used in the fitting procedure. With this in mind, we adopt the following strategy: define a chisquare function to be minimized and assign a “sigma” to each calculated result at N_{\max} that is based on the change in the calculated energy from energy at the next lowest N_{\max} value. To complete these sigma assignments, the sigma for the first point on the N_{\max} curve (the point at the lowest of the 4 N_{\max} values) is assigned a value three times the sigma calculated for the next higher N_{\max} point on the same fixed- $\hbar\Omega$ trajectory.

As a final element to our extrapolation A strategy, we invoke the minimization principle to argue that all curves of results at fixed $\hbar\Omega$ will approach the same exact answer from above. Thus all curves will have a common asymptote and we use that condition as a constraint on the chisquare minimization.

When we use exponential fits constrained to have a common asymptote and uncertainties based on the local slope, we obtain curves close to those in Fig. 4. The differences are difficult to perceive in a graph so we omit presenting a separate figure for them in this case. It is noteworthy that the equal weighting of the linear regression leads to a spread in the extrapolants that is modest.

The sequence of asymptotes for the ${}^4\text{He}$ ground state energy, obtained with extrapolation A, by using successive sets of 4 points in N_{\max} and performing our constrained fits to each such set of 4 points, is shown in Fig. 5. We employ the independent fits similar to those in Fig. 4 to define the uncertainty in our asymptotes. In particular, we define our uncertainty, or estimate of the standard deviation for the constrained asymptote, as one-half the total spread in the asymptotes arising from the independent fits with equal weights for each of the 4 points. In some other nuclei, on rare occasions, we obtain an outlier when the linear regression produces a residual less than 0.999 that we discard from the determination of the total spread. Also, on rare occasions, the calculated upper uncertainty reaches above the calculated upper bound. When this happens, we reduce the upper uncertainty to the upper bound as it is a strict limit.

One may worry that the resulting extrapolation tool contains several arbitrary aspects and we agree with that concern. Our only recourse is to cross-check these choices with solvable NCFM cases as we have done.⁸ We seek consistency of the constrained extrapolations as gauged by the uncertainties estimated from the unconstrained extrapolations described above. Indeed, our results such as those shown in Fig. 5, demonstrate that consistency. The deviation of any specific constrained

Table 1. Binding energies of several light nuclei from experiment (where available) and theory. The theoretical results are obtained with the JISP16 interaction in NCFC calculations as described in the text. The uncertainties in the rightmost digits of an extrapolation is quoted in parenthesis where available. The rightmost column provides the uppermost value of N_{\max} used in the quoted extrapolations.

Nucleus/property	Exp	Extrap (A)	Extrap (B)	Max(N_{\max})
${}^4\text{He}$ $ E(0^+, 0) $ [MeV]	28.296	28.299(1)	28.299(1)	18
${}^6\text{He}$ $ E(0^+, 1) $ [MeV]	29.269	28.68(12)	28.69(5)	14
${}^6\text{Li}$ $ E(1^+, 0) $ [MeV]	31.995	31.43(12)	31.45(5)	14
${}^8\text{He}$ $ E(0^+, 2) $ [MeV]	31.408	29.74(34)	30.05(60)	12
${}^{12}\text{C}$ $ E(0_1^+, 0) $ [MeV]	92.162	93.9(1.1)	95.1(2.7)	8
${}^{16}\text{O}$ $ E(0_1^+, 0) $ [MeV]	127.619	143.5(1.0)	150 (14)	8
${}^{14}\text{B}$ $ E(2^-, 2) $ [MeV]	85.42	83.7(3.1)	85.5 (2.0)	8
${}^{14}\text{F}$ $ E(2^-, 2) $ [MeV]	—	70.2 (3.5)	71.8 (2.4)	8

extrapolant from the result at the highest upper limit N_{\max} appears well characterized by the assigned uncertainty. We have carried out, and will present elsewhere, a far more extensive set of tests of our extrapolation methods.⁸

As we proceed to applications in heavier nuclei, we face the technical limitations of rapidly increasing basis space dimension. In some cases, only three points on the N_{\max} curves may be available so we introduce extrapolation B. Our extrapolation B procedure uses three successive points in N_{\max} to determine the exponential plus constant. We search for the value of $\hbar\Omega$ where the extrapolation is most stable and assign the uncertainty to be the difference in the extrapolated ground state energy from the two highest sets of points in N_{\max} . As expected, since extrapolation B uses less “data” to determine the asymptote, it has the larger uncertainty in most cases that we examined. Again, we trim the upper uncertainty, when needed, to conform to the upper bound.

We present the behavior of the asymptotes determined by extrapolations A and B for ${}^4\text{He}$ in Fig. 5 along with the experimental and upper bound energies. In this case the results are very rapidly convergent at many values of $\hbar\Omega$ producing uncertainties that drop precipitously with increasing N_{\max} as seen in the figure. We note that the uncertainties conservatively represent the spread in the asymptotes since all the extracted asymptotes are consistent with each other within the respective uncertainties. The largest N_{\max} points define the results quoted in Table 1, a ground state overbound by 3 ± 1 KeV.

4. Extrapolating the ground and excited state energies — NCFC for ${}^{12}\text{C}$ and ${}^{14}\text{F}$

In our investigations of the lightest nuclei⁸ we observe a marked correlation between binding energy and convergence rate: the more deeply bound ground states exhibit greater independence of $\hbar\Omega$ at fixed N_{\max} . Our physical intuition supports this correlation since we know the asymptotic tails of the bound state wave functions fall more slowly as one approaches a threshold for dissociation. This same intuition

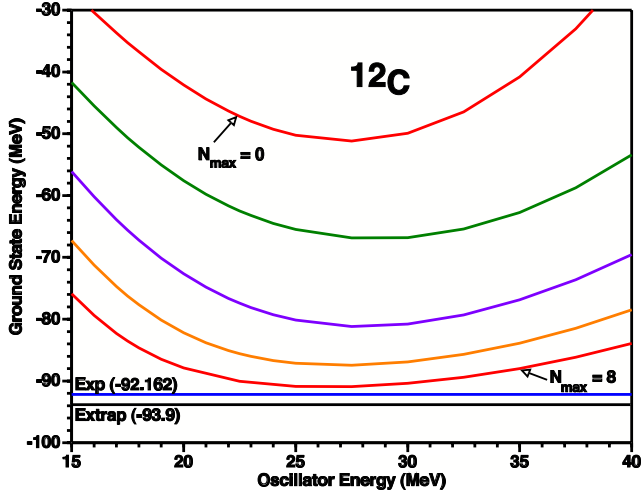


Fig. 6. (Color online) Calculated ground state energy of ^{12}C as function of the oscillator energy, $\hbar\Omega$, for selected values of N_{max} . The curve closest to experiment corresponds to the value $N_{\text{max}} = 8$ and successively higher curves are obtained with N_{max} decreased by 2 units for each curve.

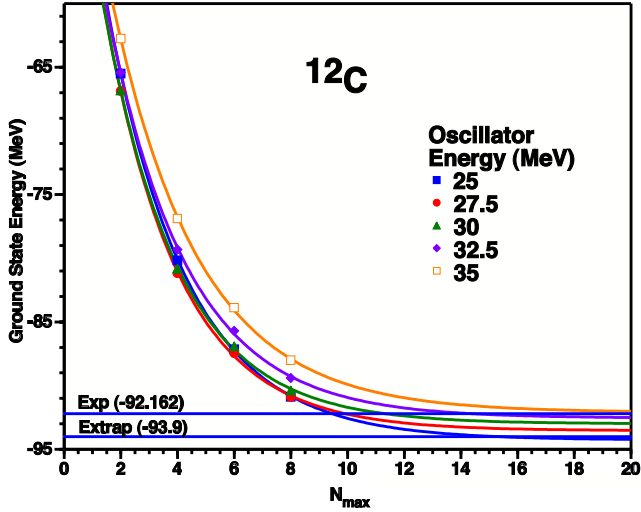


Fig. 7. (Color online) Calculated ground state energy of ^{12}C for $N_{\text{max}} = 2-8$ at selected values of $\hbar\Omega$ as described in the text. For each $\hbar\Omega$ the data are fit according to Eq. 1. The figure displays the experimental ground state energy and the common asymptote obtained in extrapolation A.

tells us to expect Coulomb barriers and angular momenta to play significant roles in this correlation.

We proceed to discuss the ^{12}C results by introducing Figs. 6 and 7. The ^{12}C nucleus is the first case for which we have only the extrapolation from the $N_{\text{max}} =$

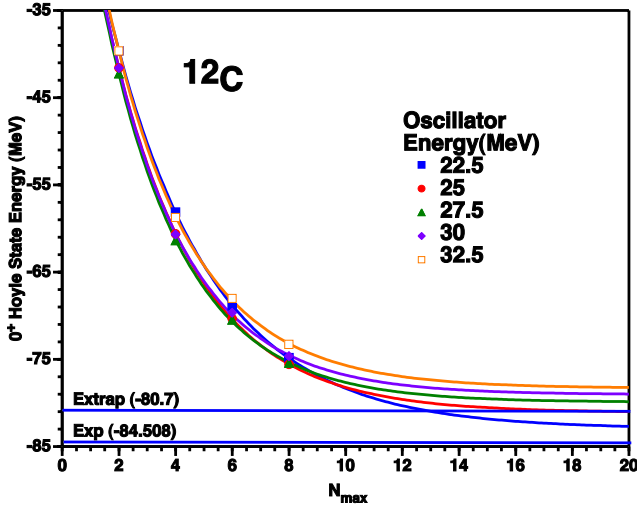


Fig. 8. (Color online) Calculated energy of ^{12}C first excited 0^+ state (Hoyle state) for $N_{\text{max}} = 2-8$ at selected values of $\hbar\Omega$ as described in the text. For each $\hbar\Omega$ the data are fit according to Eq. 1. These independent asymptotes provide a measure of our uncertainty within the global extrapolation. The figure displays the experimental energy and the common asymptote of the global extrapolation.

2–8 results since the $N_{\text{max}} = 10$ basis space, with a dimension of 7,830,355,795, is beyond our present capabilities. Thus, in order to illustrate the details of our uncertainties, we depict in Fig. 7 the linear regression analyses of our results spanning the minimum in $\hbar\Omega$ obtained at $N_{\text{max}} = 8$. Extrapolation A produces overbinding by about 1.7 MeV.

For a speculative application, we also consider the first excited 0^+ state of ^{12}C , the “Hoyle state” or “triple-alpha” state as it has come to be known. Since experimentally, this state, with $E_{\text{Hoyle}} = -84.51$ MeV, is just above the threshold for breakup into three alpha’s, $3E_{\alpha} = -84.89$ MeV, it may be poorly converged. On the other hand, our calculations for both ^6He and ^8He at $N_{\text{max}} = 2-8$ are above breakup into alpha plus neutrons, but the extrapolations from these points produce results with assessed uncertainties of about 1 MeV, and agree with our best calculations at $N_{\text{max}} = 12$.⁸ Encouraged by these results for ^6He and ^8He at $N_{\text{max}} = 8$, we apply the global extrapolation method to the first excited 0^+ state of ^{12}C . The calculated results and extrapolation are shown in Fig. 8. Our extrapolation gives $E_{\text{Hoyle}} = -80.7 \pm 2.3$ MeV, corresponding to an excitation energy of 13 ± 3 MeV, compared to an experimental excitation energy of 7.654 MeV. It remains to be seen how reliable the extrapolation is for this (and similar) states. Assuming that our assessed uncertainties are realistic, our conclusion is that JISP16 overbinds the ground state of ^{12}C by an MeV or two, but underbinds the first excited 0^+ state by about 2 to 6 MeV. When combined, we obtain an excitation energy that is too large by a significant amount.

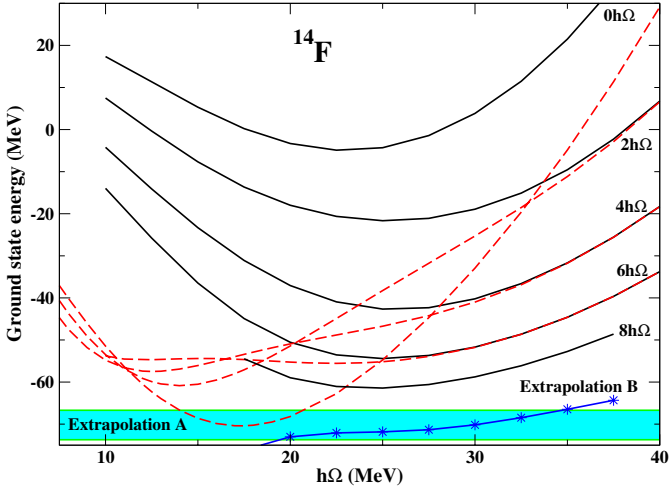


Fig. 9. (Color online) Calculated ground state energy of ^{14}F for $N_{\text{max}} = 0-8$ with “bare” (solid lines) and for $N_{\text{max}} = 0-6$ with effective (dashed lines) JISP16 interaction as function of the oscillator energy $\hbar\Omega$. Shaded area shows a confidence region of extrapolation A predictions, crosses depict predictions by extrapolation B.

Our next example is ^{14}F , an exotic neutron-deficient nucleus, the first observation of which is expected in an experiment planned in the Cyclotron Institute at Texas A&M University. In this case, we attain some results up through $N_{\text{max}} = 8$ presented in Fig. 9. The $N_{\text{max}} = 8$ basis includes about 2 billion states. In the case of extrapolation A, we obtain the binding energy prediction of 70.2 ± 3.5 MeV (shaded area in Fig. 9) which is seen to be in a good correspondence with extrapolation B. It is interesting that, contrary to our approach based on the bare JISP16 interaction, the trend of the conventional effective interaction calculations of the binding energy in the NCSM is misleading here: the minimum of the respective $\hbar\Omega$ dependence is seen from Fig. 9 to shift up with increasing N_{max} indicating the development of a shallow minimum at $N_{\text{max}} = 6$ around $\hbar\Omega = 12.5$ MeV; the ground state energy at this minimum is above the upper bound resulting from the variational principle and the $N_{\text{max}} = 8$ calculations with the bare JISP16 interaction.

In order to gauge the reliability of our prediction for the binding energy of ^{14}F , we performed similar calculations for the binding energy of ^{14}B where the experimental result is known. The resulting binding energies are presented in Table 1 along with a set of our results for additional light nuclei. Since the experimental and NCSM binding energies for ^{14}B are within our assessed uncertainty for extrapolation A, we have additional confidence in our prediction for ^{14}F binding energy. Note also the consistency between the results of extrapolations A and B.

We also performed calculations of the excited states in ^{14}F . The results obtained with $\hbar\Omega = 25$ MeV in the range of N_{max} values of 0–8, are presented in Fig. 10. We performed also the extrapolation B for the energies of these states. The respective

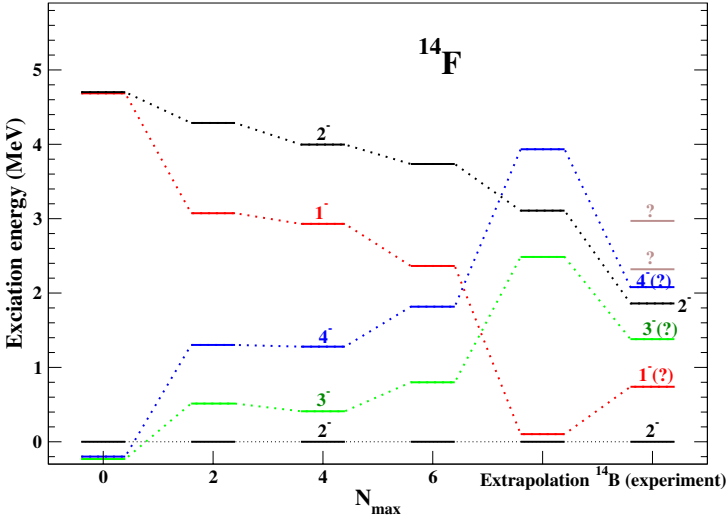


Fig. 10. (Color online) The ^{14}F spectrum obtained with $N_{\text{max}} = 0-6$ and $\hbar\Omega = 25$ MeV and by the extrapolation of the excited states in comparison with the spectrum of the mirror nucleus ^{14}B .

excitation energies, i.e. the differences between the extrapolated energies and the extrapolated ground state energy, are also shown in the figure. The ^{14}F spectrum is seen to be in a reasonable agreement with the spectrum of the mirror nucleus ^{14}B . However we should note here that the spin assignments of nearly all states in the ^{14}B spectrum are doubtful.

Clearly, much work needs to be done to come to firm predictions for the ^{14}F spectrum. These $N_{\text{max}} = 8$ calculations require tens of thousands of processors to achieve the lowest ten converged eigenvalues, eigenvectors and a suite of electromagnetic and weak observables. Such calculations represent significant investments of computational resources but are worthwhile in light of the investments needed to mount the experiments for this nucleus that sits beyond the proton drip line.

5. Conclusions and Outlook

We present in Table 1 a summary of the extrapolations performed with methods introduced here and compare them with the experimental results. In all cases, we used the calculated results to the maximum N_{max} available with the bare JISP16 interaction. In the cases of the lightest nuclei, the extrapolations were rather modest as nearly converged results were obtained directly. The assessed uncertainties apply to the least significant digits quoted in the table.

Our overall conclusion is that these NCFC results demonstrate sufficient convergence is achieved for ground state energies of light nuclei allowing extrapolations to the infinite basis limit and assessments of their uncertainties. These convergence properties reflect the soft short range behavior of the JISP16 NN interaction.

Fortunately, new renormalization schemes have been developed and applied that show promise for providing suitable nuclear Hamiltonians based on other interactions with good convergence properties within the NCFC method.⁹ Additional work is needed to develop the corresponding NNN interactions. Also, further work is in progress to extrapolate the RMS radii.

Acknowledgments

We thank Richard Furnstahl, Petr Navrátil, Vladilen Goldberg, Miles Aronmax and Christian Forssen for useful discussions. This work was supported in part by the US Department of Energy Grants DE-FC02-07ER41457 and DE-FG02-87ER40371. Results are obtained through grants of supercomputer time. This research used resources of the National Energy Research Scientific Computing Center, which is supported by the Office of Science of the U.S. Department of Energy under Contract No. DE-AC02-05CH11231. We also used Oak Ridge National Laboratory resources which are obtained under the auspices of an INCITE award (David Dean, PI). We especially wish to acknowledge MFDn code improvements¹⁰ developed in collaboration with Masha Sosonkina (Ames Laboratory), Hung Le (Ames Laboratory), Anurag Sharda (Iowa State University), Esmond Ng (LBNL), Chao Yang (LBNL) and Philip Sternberg (LBNL).

References

1. S. Weinberg, *Physica* **96A** (1979) 327; *Phys. Lett. B* **251** (1990) 288; *Nucl. Phys. B* **363** (1991) 3.
2. C. Ordonez, L. Ray and U. van Kolck, *Phys. Rev. Lett.* **72** (1994) 1982; *Phys. Rev. C* **53** (1996) 2086.
3. D. R. Entem and R. Machleidt, *Phys. Rev. C* **68** (2003) 041001(R).
4. P. Navrátil, V. G. Gueorguiev, J. P. Vary, W. E. Ormand and A. Nogga, *Phys. Rev. Lett.* **99** (2007) 014315.
5. P. Navrátil, J. P. Vary and B. R. Barrett, *Phys. Rev. Lett.* **84** (2000) 5728; *Phys. Rev. C* **62**, 054311 (2000).
6. A. M. Shirokov, J. P. Vary, A. I. Mazur and T. A. Weber, *Phys. Letts. B* **644**, 33 (2007); additional documentation and software that provides the matrix elements of the JISP16 interaction may be downloaded from nuclear.physics.iastate.edu T. A. Weber, *Phys. Lett. B* **621**, 96 (2005).
7. J. P. Vary, “The Many Fermion Dynamics Shell Model Code,” Iowa State University, 1992 (unpublished); J. P. Vary and D. C. Zheng, *ibid* 1994 (unpublished); sample runs of the code may be performed by accessing <http://nuclear.physics.iastate.edu>
8. P. Maris, J. P. Vary and A. M. Shirokov, arXiv: 0808.3420 [nucl-th], to be published.
9. S. K. Bogner, R. J. Furnstahl, P. Maris, R. J. Perry, A. Schwenk and J. P. Vary, *Nucl. Phys. A* **801** (2008) 21.
10. P. Sternberg, E. G. Ng, C. Yang, P. Maris, J. P. Vary, M. Sosonkina and H. V. Le, “Accelerating Configuration Interaction Calculations for Nuclear Structure”, Ó, in Proceedings of the 2008 ACM/IEEE Conference on Supercomputing (Austin, Texas, November 15–21, 2008). Conference on High Performance Networking and Computing. IEEE Press, Piscataway, NJ, 1-12. <http://doi.acm.org/10.1145/1413370.1413386>